

Can giant planets form by gravitational fragmentation of discs?

Radiative hydrodynamic simulations of the inner disc region

D. Stamatellos & A. P. Whitworth

School of Physics and Astronomy, Cardiff University, 5 The Parade, Cardiff CF24 3AA, Wales, UK
e-mail: D.Stamatellos@astro.cf.ac.uk
e-mail: A.Whitworth@astro.cf.ac.uk

Received September, 2007; accepted

ABSTRACT

Context. Disc fragmentation has been proposed as a possible mechanism for the formation of giant planets at close distances to solar-type stars. However, it is debatable whether this mechanism can function in the inner region of real discs.

Aims. To investigate the thermodynamics of discs and the probability of fragmentation.

Methods. We use a newly developed method to treat the energy equation and equation of state, which accounts for radiative transfer effects in SPH simulations of protostellar discs. The different chemical and internal states of hydrogen and the properties of dust at different densities and temperatures (ice coated dust grains at low temperatures, ice melting, dust sublimation) are all taken into account by the new method.

Results. We present radiative hydrodynamic simulations of discs where the effects of the equation of state and energy equation are taken into account. We focus on the inner parts of discs, $R < 40$ AU and examine 2 cases (i) a disc heated by an ambient radiation field of 10 K, and (ii) a disc with additional heating from the central star. In both cases the disc does not fragment; in the former case because it cannot cool fast enough, and in the latter case because it is not gravitationally unstable. Our results corroborate the results of Boley et al. (2006) and Cai et al. (2007), who use a different treatment for the radiative transfer.

Conclusions. Disc fragmentation is unlikely to be able to produce giant planets around solar-type stars at radii $\lesssim 50$ AU.

Key words. Accretion, accretion discs – Hydrodynamics – Instabilities – Radiative Transfer – Planetary systems: formation – Planetary systems: protoplanetary discs

1. Introduction

A large number of exoplanets (~ 250) has been discovered around nearby stars in the last 12 years, mainly with the radial velocity method. Most of these exoplanets have properties that are different from those of the Solar System. In particular, giant planets are found very close to the central star on orbits of apparently random eccentricity.

Two main theories have been proposed for the formation of giant planets, (i) core accretion, and (ii) gravitational fragmentation. In the core accretion scenario giant planets form by coagulation of planetesimals (e.g. Safronov 1969; Goldreich & Ward 1973; Pollack et al. 1996). Once a solid body of around $10 M_{\oplus}$ is reached, it quickly accretes a large gaseous envelope. One of the main problems of this theory is that the timescale for planet formation is long. The theory predicts that planets can form within a few million years, but observations suggest that circumstellar discs may not be that long lived (Haisch, Lada & Lada 2001; Cieza et al. 2007). In the gravitational fragmentation scenario, giant planets form by gravitational instability in massive discs (e.g. Kuiper 1951; Cameron 1978; cf. review by Durisen et al. 2007). The main advantage of this method is

that planets form on a dynamical timescale, i.e. within a few hundred years.

There are two conditions that must be fulfilled for discs to fragment gravitationally. (i) The disc must be gravitationally unstable, i.e. massive enough so that gravity can overcome thermal pressure and centrifugal support (Toomre 1964):

$$Q(R) = \frac{c(R)\kappa(R)}{\pi G \Sigma(R)} \lesssim 1, \quad (1)$$

where c is the sound speed, κ is the epicyclic frequency, and Σ is the surface density. (ii) The disc must be able to cool fast enough for the compressional energy provided by the collapse to be radiated away. Theory and simulations (Gammie 2001; Johnson & Gammie 2003; Rice et al. 2003, 2005; Mayer et al. 2004; Mejia et al. 2005) indicate that the disc cooling must happen on a dynamical time-scale,

$$t_{\text{COOL}} < C(\gamma)t_{\text{ORB}}, \quad 0.5 \lesssim C(\gamma) \lesssim 2.0, \quad (2)$$

where t_{ORB} is the period and γ is the adiabatic exponent.

However, it is uncertain whether *real discs* actually satisfy the above conditions. Boss (2004) and Mayer et al. (2007)

suggest that convection can provide sufficiently fast cooling, whereas Johnson & Gammie (2003), Boley et al. (2006) and Nelson (2006), assert that there is no efficient cooling mechanism, and hence fragmentation is not possible. The latter point of view is supported by analytic studies which suggest that convection cannot provide the required cooling (Rafikov 2007; Whitworth et al. 2007), and that discs cannot cool fast enough, at least close ($R \lesssim 50$ AU) to the central star (Rafikov 2005; Matzner & Levin 2005; Whitworth & Stamatellos 2006).

Hydrodynamic simulations have produced contradictory results about whether disc fragmentation can produce giant planets close to the central star, mainly due the different treatments of radiative transfer in discs. We have recently developed an efficient scheme to capture the thermal and radiative effects when protostellar gas fragments (see Section 2 and Stamatellos et al. 2007). Thus, we are able for the first time to perform radiative hydrodynamic simulations of discs where the effects of the equation of state are included. Moreover the radiative scheme allows to include irradiation of the disc by the central star.

The structure of the paper is as follows. In Section 2 we describe the method that is used for the radiative hydrodynamic simulations. In Section 3 we describe the disc initial setup and in Section 4 the radiative hydrodynamic simulations. Finally, in Section 5 we discuss the results of these simulations and their implications for the possibility of forming giant planets close to a star by gravitational fragmentation.

2. Numerical method

For the simulations we use the SPH code DRAGON (Goodwin et al. 2004), which invokes an octal tree (to compute gravity and find neighbours), adaptive smoothing lengths, multiple particle timesteps, artificial viscosity ($\alpha = 0.1, \beta = 0.2$) with the Balsara switch, and a second-order Runge-Kutta integration scheme.

The energy equation is treated with the method of Stamatellos et al. (2007). The method takes into account compressional heating, viscous heating, radiation heating from the background, radiation cooling and, implicitly, radiation heating from the particle's neighbourhood. It performs well, both in the optically thin and optically thick regime, and it is efficient and relatively easy to implement in particle- and grid-based codes.

The gas is assumed to be a mixture of hydrogen and helium. We use an equation of state (Black & Bodenheimer 1975; Masunaga et al. 1998; Boley et al. 2007) that accounts (i) for the rotational and vibrational degrees of freedom of molecular hydrogen, and (ii) for the different chemical states of hydrogen and helium depending on the temperature and density, i.e. the effects of H_2 dissociation, H^0 ionisation, and the first and second ionisation of He are included. Hence, the effects of variations in the equation of state are taken into account. (We note however that (i) the temperatures in the simulations presented here are not high enough for the molecular hydrogen to dissociate, and (ii) contributions from metals are ignored; hence the gas composition remains the same, i.e. the mean molecular weight μ is constant).

For the dust and gas opacity we use the parameterization by Bell & Lin (1994), $\kappa(\rho, T) = \kappa_0 \rho^a T^b$, where κ_0, a, b are constants that depend on the species and the physical processes contributing to the opacity at each ρ and T . The opacity changes due to e.g. ice mantle melting, the sublimation of dust, molecular and H^- contributions, are all taken into account.

The code has been extensively tested (see Stamatellos et al. 2007). In particular it reproduces the detailed 3D results of Masunaga & Inutsuka (2000) and the analytic test of Spiegel (1957). We report a further test here in Section 4.1.2.

3. Disc initial conditions

We simulate a $0.07 M_\odot$ disc around a $0.5 M_\odot$ star. This is a relatively massive disc but such discs have been observed e.g. in the Orion Nebula cluster (Eisner & Carpenter 2006). The disc initially extends from 2 to 40 AU. Its initial surface density is $\Sigma(R) \sim R^{-1/2}$ and its initial temperature is $T(R) \sim R^{-1}$. These are typical density and temperature profiles of discs and have been chosen so as to match the initial conditions of the simulations of Boley et al. (2006) and Cai et al. (2007).

More specifically we assume a disc surface profile

$$\Sigma(R) = \Sigma_0 R^{-1/2}, \quad (3)$$

where $\Sigma_0 = 1.6 \times 10^3 \text{ g cm}^{-2}$, and R denotes the distance from the rotation axis. The disc temperature profile is

$$T_d(R) = \left[T_0^2 \left(\frac{R}{\text{AU}} \right)^{-2} + T_\infty^2 \right]^{1/2}. \quad (4)$$

$T_0 = 1200$ K is the temperature at $R \simeq 1$ AU and $T_\infty = 10$ K is the asymptotic temperature far from the central star.

To calculate the initial thickness $z_0(R)$ of the disc, we balance the vertical component of the gravitational force of the star and the gravitational force of the underlying disc, against the pressure force due to the disc temperature (disc thermal pressure):

$$\frac{GM_\star}{R^2} \frac{z_0(R)}{R} + \pi G \Sigma(R) \approx \frac{c^2(R)}{z_0(R)}, \quad (5)$$

where $c^2(R) = kT(R)/(\mu m_p)$ is the local sound speed. The above equation can be written as

$$\frac{GM_\star}{R^3} z_0^2(R) + \pi G \Sigma(R) z_0(R) - c^2(R) = 0, \quad (6)$$

which is a simple quadratic equation with a positive root

$$z_0(R) = -\frac{\pi \Sigma(R) R^3}{2M_\star} + \left[\left(\frac{\pi \Sigma(R) R^3}{2M_\star} \right)^2 + \frac{R^3}{GM_\star} c^2(R) \right]^{1/2} \quad (7)$$

4. Simulations

We perform 2 disc simulations; (i) one without stellar irradiation but with a constant background radiation field of $T_{\text{BGR}} = 10$ K (cf. Boley et al. 2006; Cai et al. 2007), and (ii) one with radiation from the central star ($T_{\text{BGR}} \sim R^{-1}$). We use 2×10^5 SPH particles to represent the disc. In both cases the disc relaxes from the initial conditions to a quasi-steady state. In Fig. 1 we

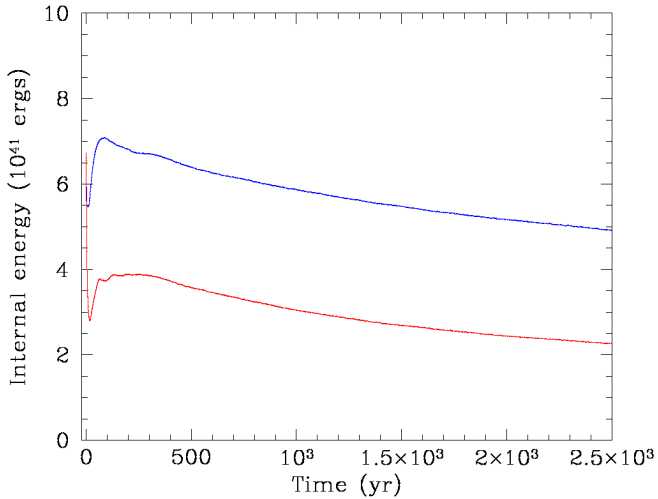


Fig. 1. Internal energy of the disc (i) for a disc under low background heating ($T_{\text{BGR}} = 10$ K; bottom, red line) and (ii) for a disc irradiated by the central star ($T_{\text{BGR}}(R) \sim R^{-1}$; top, blue line).

plot the evolution of the disc internal energy with time for both cases. When the heating from the central star is ignored the disc relaxes to a lower-temperature quasi-steady state (bottom line) than in the case when irradiation by the star is taken into account (top line). Otherwise the evolution of the thermal energy appears similar in both cases. In the next subsections we describe in detail the characteristics of each simulation.

4.1. Disc evolution under low background heating ($T_{\text{BGR}} = 10$ K)

We assume a constant background radiation field of $T_{\text{BGR}} = 10$ K. The disc relaxes to a quasi-steady state (or “asymptotic phase”; cf. Boley et al. 2006) within ~ 250 yr. Thereafter, the disc cools slowly. Weak spiral arms form in the disc but they do not show any tendency to fragment (cf. Fig 2), despite the fact that the disc is Toomre unstable at $\sim 30 - 35$ AU (Fig 4). This is because the disc cannot cool fast enough; the cooling time throughout the disc is generally $\gtrsim 2t_{\text{ORB}}$ (Fig. 5), where t_{ORB} is the local orbital period.

In Figs. 6 and 7 we plot the azimuthally averaged surface density, temperature, Toomre parameter Q , and cooling time (in units of the local orbital period). The temperature and cooling time are additionally averaged vertically relative to the disc midplane. The Toomre parameter is calculated using the surface density and the midplane disc temperature. Each plot contains 5 lines that correspond to different instances during the disc evolution ($t = 500, 1000, \dots, 2500$ yr). The profiles are essentially independent of the time, i.e. the disc is in a quasi-steady state, while it slowly cools (see temperature profile in Fig. 6).

This simulation was repeated using a smaller number of SPH particles (5×10^4) and the evolution of the thermal energy, surface density, temperature, Toomre parameter and cool-

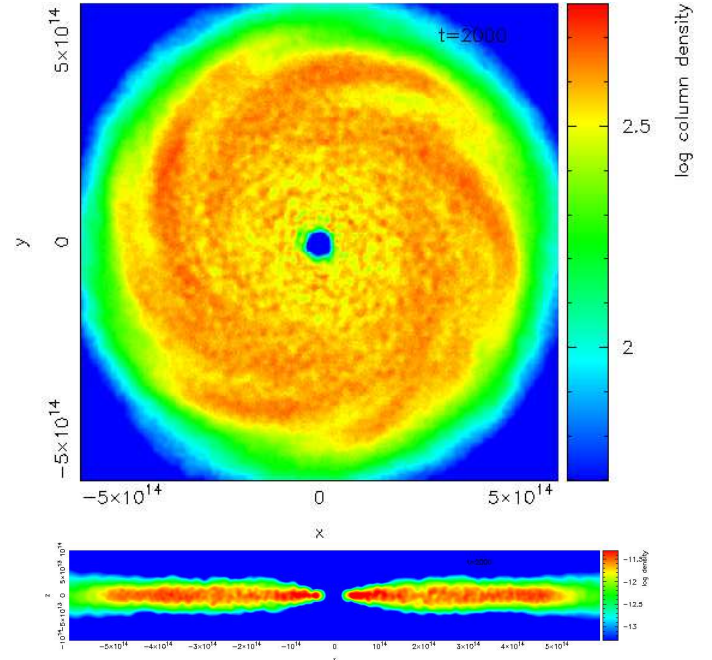


Fig. 2. Logarithmic column density (top) and cross-section of the density on the x-z plane (bottom) for a disc heated by a low-temperature background radiation field of $T_{\text{BGR}} = 10$ K. x and y are given in cm.

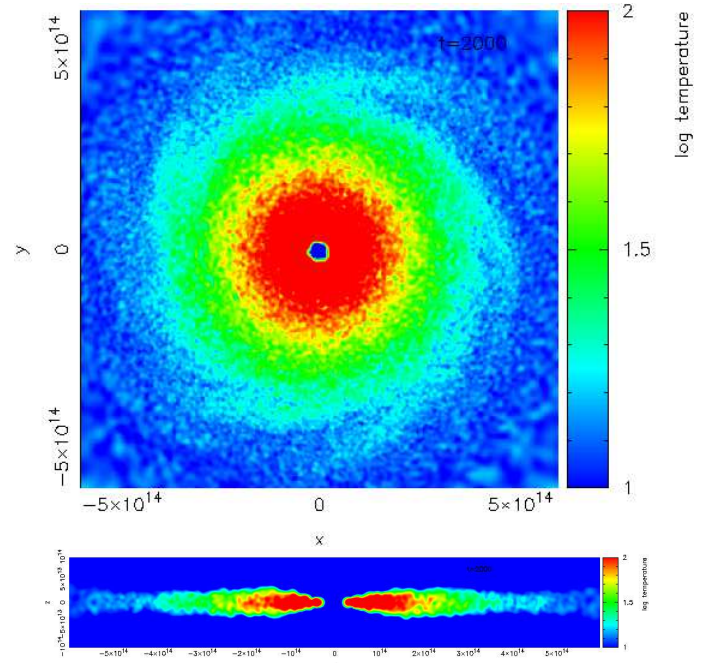


Fig. 3. Logarithmic temperature in the x-y plane (top) and on the x-z plane (bottom) for a disc heated by a low-temperature background radiation field of $T_{\text{BGR}} = 10$ K.

ing time were essentially the same. The profiles change only slowly with time as the disc cools quasi-statically.

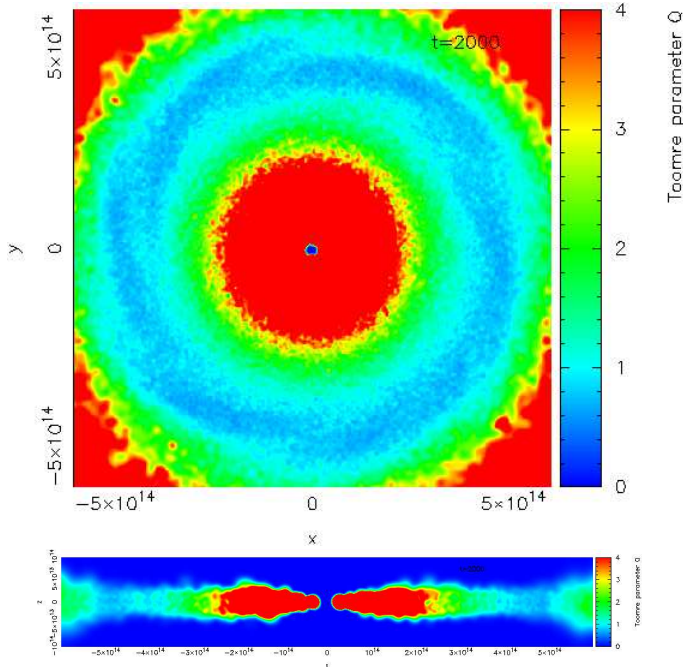


Fig. 4. Toomre parameter in the x-y plane (top) and on the x-z plane (bottom) for a disc heated by a low-temperature background radiation field of $T_{BGR} = 10$ K.

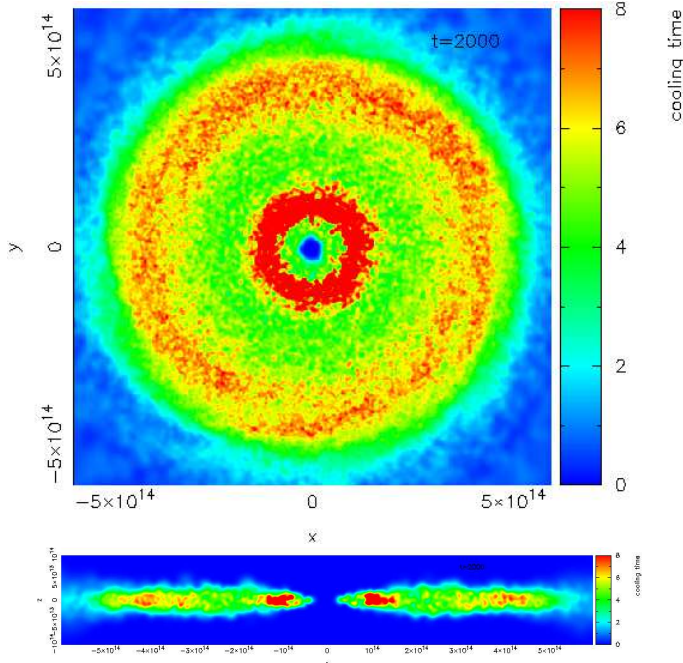


Fig. 5. Cooling time (in units of the local orbital period) in the x-y plane (top) and on the x-z plane (bottom) for a disc heated by a low-temperature background radiation field of $T_{BGR} = 10$ K.

4.1.1. Comparison with the simulations of Boley et al. (2006) and Cai et al. (2007)

The spiral arms that develop in the disc are weaker than those reported by Boley et al. (2006). The temperatures that are calculated are generally larger than those of Boley et al. (2006).

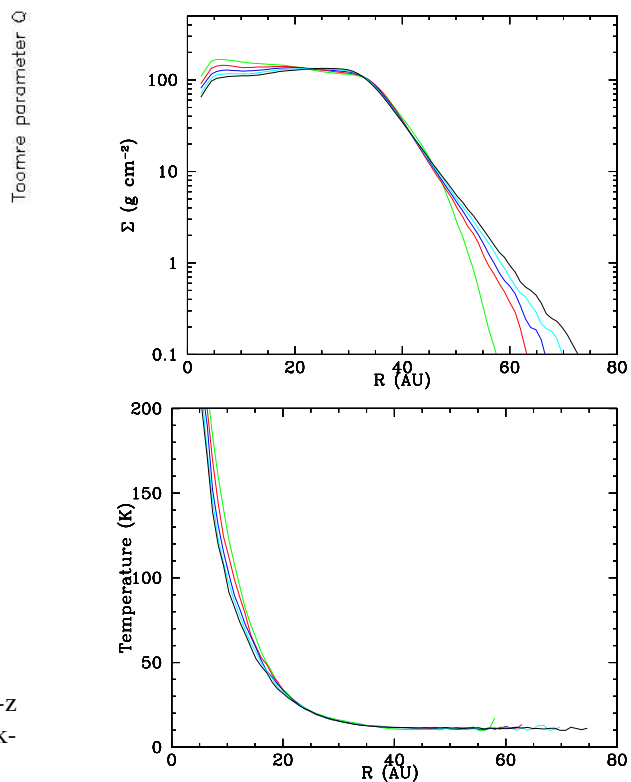


Fig. 6. Surface density (azimuthally averaged) and temperature (azimuthally and vertically averaged) at 5 instances during the disc evolution ($t = 500, 1000, \dots, 2500$ yr; green, red, blue, cyan, black).

These differences at large radii (≥ 30 AU) are attributable to using a different background radiation field; in our simulation $T_{BGR} = 10$ K whereas in Boley et al. simulations the disc can cool down to 3 K. At small radii they could be due to higher viscous heating in our simulations. By comparing the internal energies between the two simulations we estimate that the temperatures we calculate are $\sim 15\%$ higher. However, considering the differences between the radiative transfer schemes and between the hydrodynamic methods (SPH versus grid-based) the reported discrepancies are rather small. The Toomre parameter in this simulation is generally higher than that of Boley et al. (2006) but the cooling times are lower. This is due to the higher temperatures in our simulation ($Q \propto T^{0.5}$, $t_{COOL} \propto T^{-3}$). Both simulations show no sign or even any tendency to fragment.

The results of our simulation are more comparable to the results of the simulation by Cai et al. (2007) with external envelope irradiation of 15 K. The strength of the spiral arms in our simulation are similar to their simulation. The estimated temperatures across the disc are also similar; by comparing the internal energies we estimate that the temperatures that we calculate are less than 3% higher than those reported by Cai et al. (2007). Both simulations show no tendency towards fragmentation.

We conclude that both the Indiana University Hydrodynamics Group code (e.g. Pickett et al. 1998; Mejia et al. 2005) and our SPH-RT code produce very similar results,

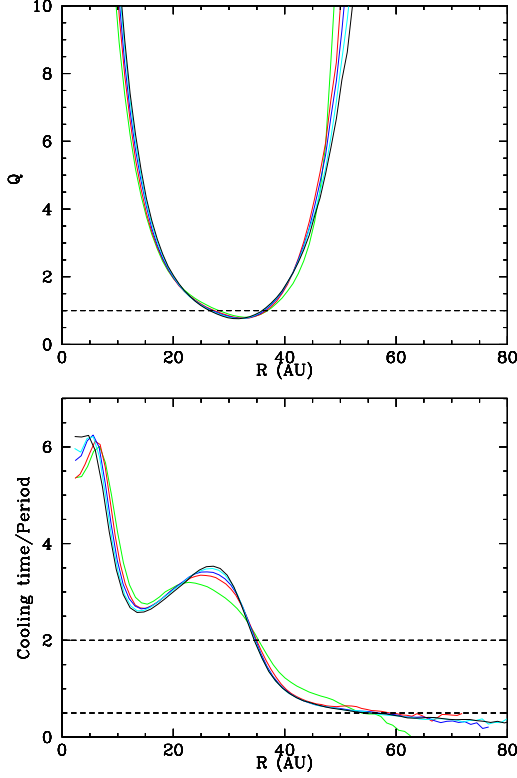


Fig. 7. Toomre parameter (azimuthally averaged) and cooling time (in units of the local orbital period; also azimuthally averaged) at 5 instances during the disc evolution (as in Fig. 6).

which is reassuring since the treatment of radiative transfer and hydrodynamics are completely different.

4.1.2. The vertical temperature profile of the disc; comparison with analytic calculations

The radiative hydrodynamic computational scheme has already been tested for the case of collapsing clouds and has been proved to perform well (Stamatellos et al. 2007). To provide a different test of this scheme for disc configurations, we compare our results with the analytic calculations of Hubeny (1990) (cf. Boley et al. 2007).

Hubeny (1990) studies the vertical structure of a cylindrically symmetric stationary keplerian disc. The radiation transport is treated only in the direction vertical to the disc midplane. The energy is provided by the shear viscosity of the Keplerian motion, whereas the self-gravity of the disc is neglected. Convection and external irradiation are also neglected. If it is further assumed that the viscosity is independent of the depth in the disc then Hubeny's LTE gray solution for the temperature T at optical depth τ from the surface of the disc approximates to

$$T(\tau) = T_{\text{eff}} \left\{ \frac{3}{4} \left[(\tau - \tau_{\theta}) + \frac{1}{\sqrt{3}} \right] + \frac{1}{3\kappa(\tau)\Sigma} \right\}^{1/4}, \quad (8)$$

where σT_{eff}^4 is the flux at the disc midplane, perpendicular to this plane, Σ is the column density from the surface of the disc

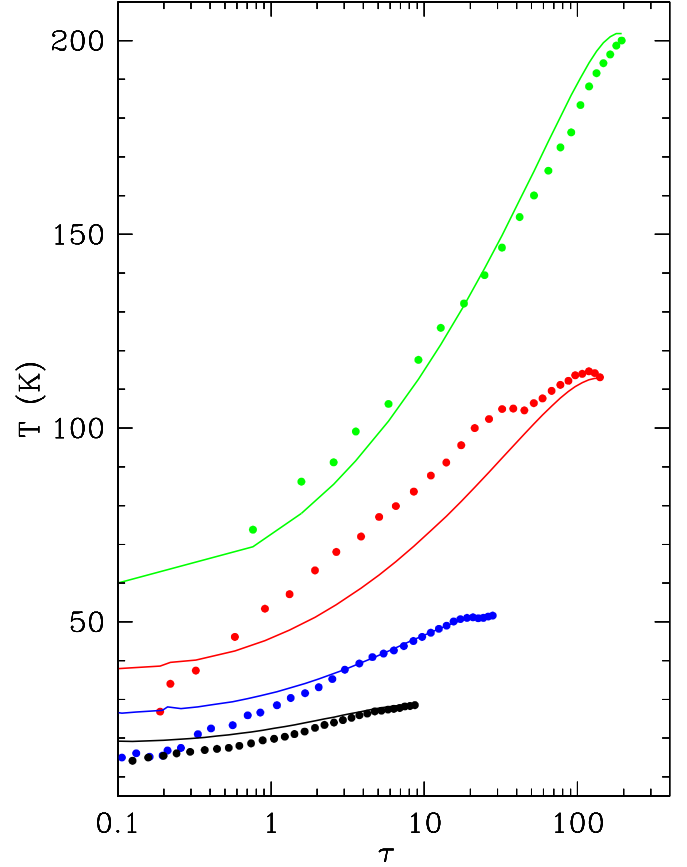


Fig. 8. Disc temperature profiles vertically to the disc midplane at different radii from the central star (6, 10, 15, and 20 AU, top to bottom). The temperature T is plotted as a function of the vertical optical depth τ from the surface to the midplane of the disc. Points correspond to the results of our model (azimuthally averaged) and the lines to the Hubeny (1990) analytic model.

to the disc midplane, $\tau_{\theta} = \int_0^{\sigma} \kappa(\sigma') \sigma' d\sigma'$, where $\kappa(\sigma)$ is the mass opacity and $\sigma(z) = \int_z^{\infty} \rho dz$

To satisfy the assumption of a disc in equilibrium we compare the Hubeny (1990) analytic calculation with a snapshot of the disc at $t = 2000$ yr, i.e. during the quasi-steady state. There are spiral arms in the disc but they are relatively weak and they should not affect the results of this calculation. However, we note that this simulation accounts for external disc irradiation by a background field of 10 K and for the disc self-gravity. Hence, we expect that the vertical temperature profile of the disc should be similar to the one provided by Hubeny (1990) (Eq. 8), but a bit warmer due to these additional heating sources.

In Fig. 8 we present the vertical temperature structure at different radii from the central star (6, 10, 15, and 20 AU, top to bottom). In this graph the temperature is plotted as a function of the vertical optical depth from the surface to the midplane of the disc. As expected our temperature profiles are similar to those predicted by Hubeny (1990). There are some deviations

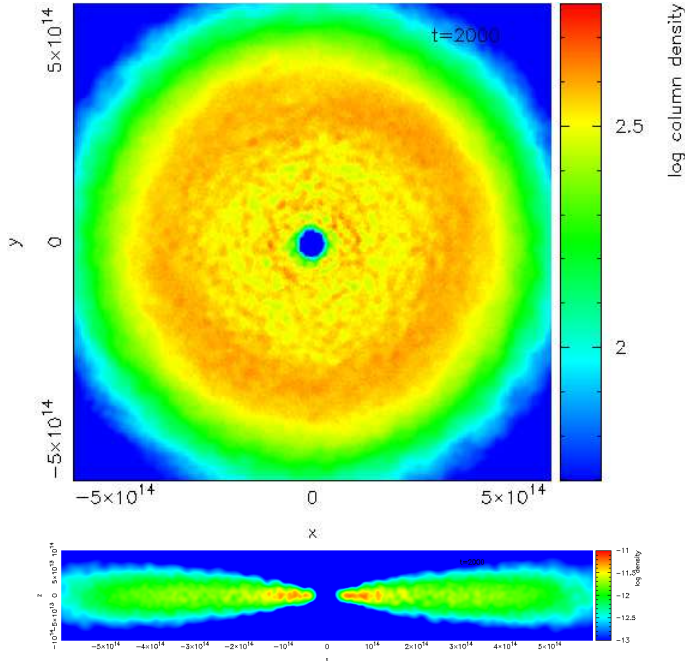


Fig. 9. Logarithmic column density (top) and cross-section of the density on the x - z plane (bottom) for a disc heated by the central star.

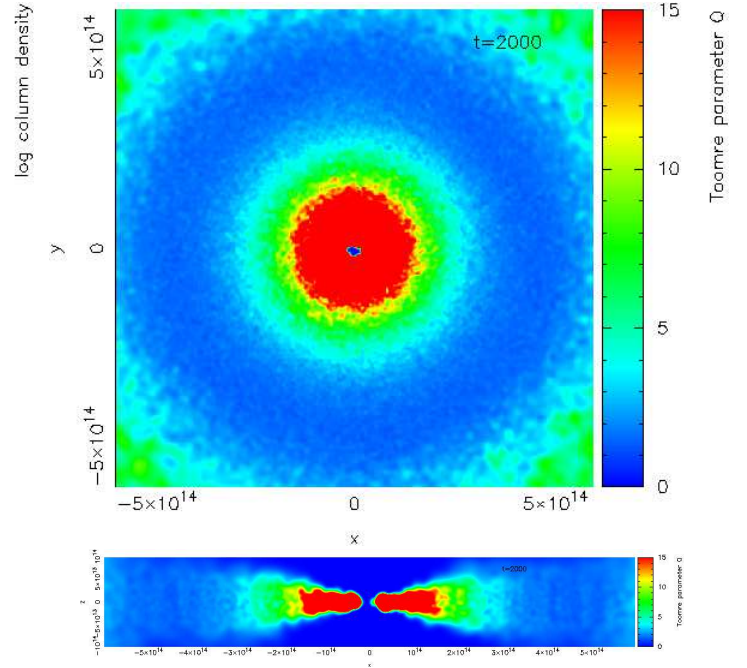


Fig. 11. Toomre parameter the x - y plane (top) and on the x - z plane (bottom) for a disc heated by the central star.

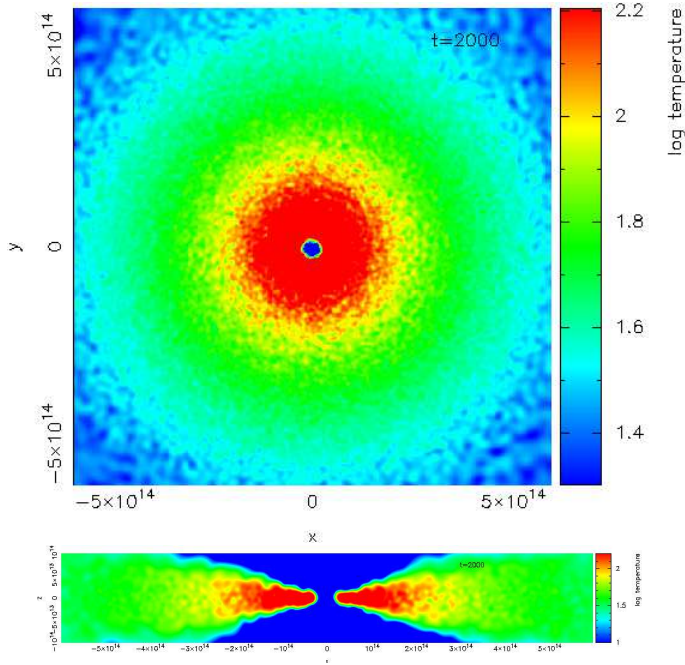


Fig. 10. Logarithmic temperature in the x - y plane (top) and on the x - z plane (bottom) for a disc heated by the central star.

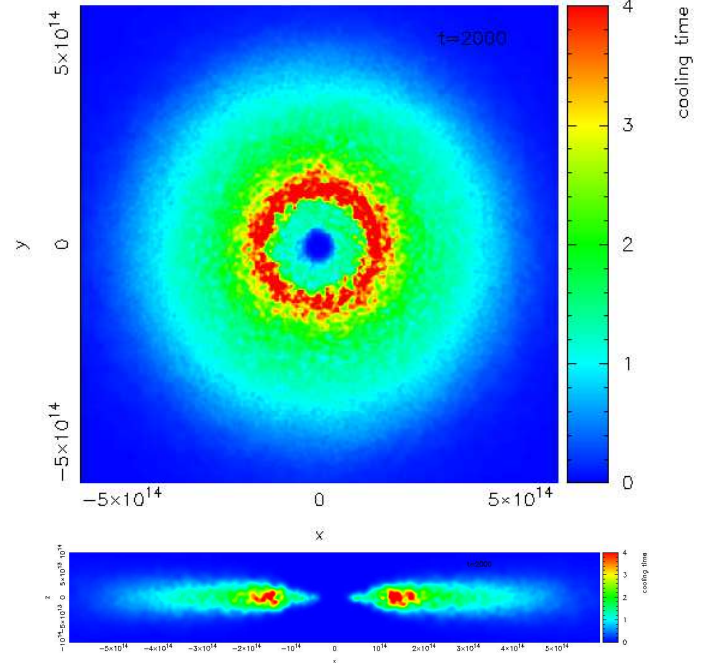


Fig. 12. Cooling time (in units of the local orbital period) in the x - y plane (top) and on the x - z plane (bottom) for a disc heated by the central star.

4.2. Disc evolution with stellar heating

We take into account radiation from the central star by assuming the background temperature is

at larger distances from the central star at low optical depths; in our simulation the disc surface cools more efficiently.

$$T_{\text{BGR}}(R) = \left[T_0^2 \left(\frac{R}{\text{AU}} \right)^{-2} + T_\infty^2 \right]^{1/2}, \quad (9)$$

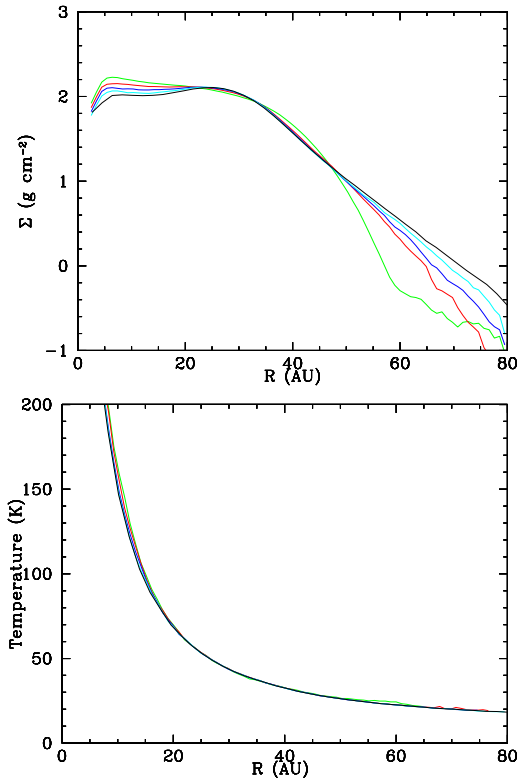


Fig. 13. Surface density (azimuthally averaged) and temperature (azimuthally and vertically averaged) at 5 instances during the evolution of a disc heated by the central star ($t = 500, 1000, \dots, 2500$ yr; green, red, blue, cyan, black).

where $T_0 = 1200$ K and $T_\infty = 10$ K (cf. Eq. 4). The results of this simulation are shown in Figs. 9-14. In this case the initial conditions of the disc are closer to equilibrium, hence the temperature of the disc remains almost constant (see Fig. 13). The disc is overall hotter than in the previous case due to heating from the central star. Due to higher temperature the disc cools fast enough to fragment at radii ≥ 20 AU (Fig. 14). However, it does not fragment as it is not gravitationally unstable $Q \geq 1.5$ K (Fig. 14).

The effect of the heating from the central star is to stabilize the disc; in this case the disc appears axisymmetric with no signs of spiral arms. This result is consistent with previous simulations of discs heated by “envelope-radiation”, i.e. by an isotropic background radiation field (Boss 2001, 2002; Cai et al. 2007), and with analytical calculations (Matzner & Levin 2005; Rafikov 2005; Whitworth & Stamatellos 2006).

5. Discussion

We have performed radiative hydrodynamic simulations of the inner region of circumstellar discs with initial parameters similar to the parameters of Boley et al. (2006) and Cai et al. (2007), i.e. a $0.07 M_\odot$ disc around a $0.5 M_\odot$ star. The disc initially extends from 2 to 40 AU. The disc initial surface density is $\Sigma(R) \sim R^{-1/2}$ and the disc initial temperature is $T(R) \sim R^{-1}$. We use a newly developed method to treat the energy equation in SPH simulations of discs and an equation of state that includes

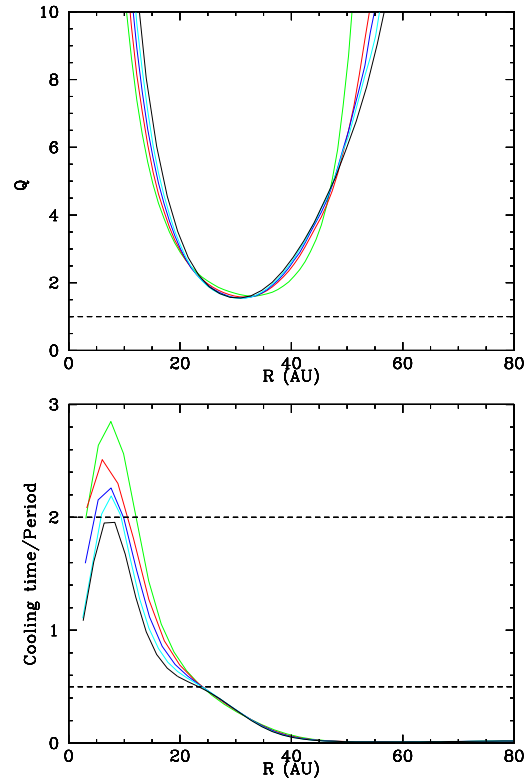


Fig. 14. Azimuthally averaged Toomre parameter and cooling time (in units of the local orbital period) at 5 instances the evolution of a disc heated by the central star (as in Fig. 6).

the effects of the rotational degrees of freedom of molecular hydrogen and realistic dust opacities.

Initially we simulated the evolution of the disc under an external radiation field of temperature 10 K. Our results are comparable with the results of Boley et al. (2006) and Cai et al. (2007); the disc is gravitationally unstable at $R \sim 20 - 30$ AU, but it does not fragment because it cannot cool fast enough. Spiral arms form in the disc but they are weak and do not show any tendency towards fragmentation. The adiabatic index is $\gamma = 5/3$ outside ~ 10 AU where the temperature is less than ~ 80 K; however closer to the central star where the temperature is higher, $\gamma = 7/5$, due to the excitation of the rotational degrees of freedom of molecular hydrogen. It has been suggested that when γ is decreases from $5/3$ to $7/5$, the maximum cooling time for the disc to fragment also increases from 0.5 to $2 t_{\text{ORB}}$ (e.g. Johnson & Gammie 2003; Rice et al. 2005). Our simulations indicate that in discs the cooling time is always $\geq 2 t_{\text{ORB}}$ within ~ 30 AU, hence such discs are not expected to fragment and they do not fragment. The results of the simulations reported here are similar to the results of the simulations of Boley et al. (2006) and Cai et al. (2007) despite using different treatments for the radiative transfer and for the hydrodynamics.

We also simulated the evolution of a disc in an external radiation field whose temperature drops as R^{-1} , to mimic the irradiation from the central star and envelope. In this case the disc can cool fast enough to fragment (because of its higher temperature) but it does not fragment because it is not gravi-

tationally unstable. The heating from the central star stabilizes the disc; no spiral arms form in this case. Hence, discs are even less prone to fragment in their inner regions when the effect of stellar irradiation is taken into account. This result agrees with previous simulation of discs heated by envelope radiation (Boss 2001, 2002; Cai et al. 2007). It is also in accordance with previous analytical calculations (Matzner & Levin 2005; Rafikov 2005; Whitworth & Stamatellos 2006). Whitworth & Stamatellos (2006) argue fragmentation is possible at larger distances (≥ 100 AU) from the central star where the cooling times are sufficiently short. However, their results suggest that fragmentation at large radii produces mostly brown dwarfs and occasionally low-mass hydrogen-burning stars or planetary-mass objects (Whitworth & Stamatellos 2006; Whitworth et al. 2007; Stamatellos, Hubber & Whitworth 2007). If planetary mass objects form at such large radii they are unlikely to migrate inwards to become hot Jupiters. More likely they are ejected into the field through 3-body interactions.

Hence, based on the simulations presented in this paper, we conclude that gas giant planets probably cannot form close to the central star by gravitational fragmentation of discs.

Acknowledgements. We would like to thank R. Durisen, A. Boley and K. Rice for useful discussions. The computations reported here were performed using the UK Astrophysical Fluids Facility (UKAFF). We also acknowledge support by PPARC grant PP/E000967/1.

References

- Bell, K. R., & Lin, D. N. C. 1994, *ApJ*, 427, 987
 Black, D. C., & Bodenheimer, P. 1975, *ApJ*, 199, 619
 Boley, A. C., Hartquist, T. W., Durisen, R. H., & Michael, S. 2007, *ApJ*, 656, L89
 Boley, A. C., Mejía, A. C., Durisen, R. H., Cai, K., Pickett, M. K., & D'Alessio, P. 2006, *ApJ*, 651, 517
 Boss, A. P. 2004, *ApJ*, 610, 456
 Boss, A. P. 2002, *ApJ*, 576, 462
 Boss, A. P. 2001, *ApJ*, 563, 367
 Cieza, L., et al. 2007, ArXiv e-prints, 706, arXiv:0706.0563
 Cai, K., Durisen, R. H., Boley, A. C., Pickett, M. K., & Mejia, A. C. 2007, ArXiv e-prints, 706, arXiv:0706.4046
 Cameron, A. G. W. 1978, *Moon and Planets*, 18, 5
 Durisen, R. H., Boss, A. P., Mayer, L., Nelson, A. F., Quinn, T., & Rice, W. K. M. 2007, *Protostars and Planets V*, 607
 Eisner, J. A., & Carpenter, J. M. 2006, *ApJ*, 641, 1162
 Gammie, C. F. 2001, *ApJ*, 553, 174
 Goodwin, S. P., Whitworth, A. P., & Ward-Thompson, D., 2004, *A&A*, 414, 633
 Goldreich, P., & Ward, W. R. 1973, *ApJ*, 183, 1051
 Goodwin, S. P., & Whitworth, A. 2007, *A&A*, 466, 943
 Haisch, K. E., Jr., Lada, E. A., & Lada, C. J. 2001, *ApJ*, 553, L153
 Hubeny, I. 1990, *ApJ*, 351, 632
 Johnson, B. M., & Gammie, C. F. 2003, *ApJ*, 597, 131
 Kuiper, G. P. 1951, *Proceedings of the National Academy of Science*, 37, 1
 Masunaga, H., & Inutsuka, S.-i. 2000, *ApJ*, 531, 350
 Masunaga, H., Miyama, S. M., & Inutsuka, S.-I. 1998, *ApJ*, 495, 346
 Matzner, C. D., & Levin, Y. 2005, *ApJ*, 628, 817
 Mayer, L., Lufkin, G., Quinn, T., & Wadsley, J. 2007, *ApJ*, 661, L77
 Mayer, L., Quinn, T., Wadsley, J., & Stadel, J. 2004, *ApJ*, 609, 1045
 Mejía, A. C., Durisen, R. H., Pickett, M. K., & Cai, K. 2005, *ApJ*, 619, 1098
 Nelson, A. F. 2006, *MNRAS*, 373, 1039
 Pickett, B. K., Cassen, P., Durisen, R. H., & Link, R. 1998, *ApJ*, 504, 468
 Pollack, J. B., Hubickyj, O., Bodenheimer, P., Lissauer, J. J., Podolak, M., & Greenzweig, Y. 1996, *Icarus*, 124, 62
 Rafikov, R. R. 2007, *ApJ*, 662, 642
 Rafikov, R. R. 2005, *ApJ*, 621, L69
 Rice, W. K. M., Lodato, G., & Armitage, P. J. 2005, *MNRAS*, 364, L56
 Rice, W. K. M., Armitage, P. J., Bate, M. R., & Bonnell, I. A. 2003, *MNRAS*, 339, 1025
 Safronov, V. S. 1969, *Evolution of the protoplanetary cloud and formation of the Earth and Planets* (Moscow: Nauka)
 Spiegel, E. A. 1957, *ApJ*, 126, 202
 Stamatellos, D., Hubber, D., & Whitworth, A. 2007, ArXiv e-prints, 708, arXiv:0708.2827
 Stamatellos, D., Whitworth, A. P., Bisbas, T., & Goodwin, S. 2007, ArXiv e-prints, 705, arXiv:0705.0127
 Toomre, A. 1964, *ApJ*, 139, 1217
 Whitworth, A., Bate, M. R., Nordlund, Å., Reipurth, B., & Zinnecker, H. 2007, *Protostars and Planets V*, 459
 Whitworth, A. P., & Stamatellos, D. 2006, *A&A*, 458, 817